International Journal of Concrete Structures and Materials
Vol.19, No.1E, pp.03~09, March 2007

Numerical Study on the Joints between Precast Post-Tensioned Segments

Tae-Hoon Kim[1)], Young-Jin Kim[1)], Byeong-Moo Jin[1)], and Hyun-Mock Shin[2)]

(Received August 31, 2006, Accepted January 15, 2007)

Abstract: This paper presents a numerical procedure for analyzing the joints between precast post-tensioned segments. A computer program for the analysis of reinforced concrete structures was run for this problem. Models of material nonlinearity considered in this study include tensile, compressive and shear models for cracked concrete and a model for reinforcing steel with smeared crack. An unbonded tendon element based on the finite element method, that can describe the interaction between the tendon and concrete of prestressed concrete member, was experimentally investigated. A joint element is newly developed to predict the inelastic behavior of the joints between segmental members. The proposed numerical method for the joints between precast post-tensioned segments was verified by comparison of its results with reliable experimental results.

Keywords: precast, post-tensioned segments, material nonlinearity, unbonded tendon element, joint element

1. Introduction

The use of precast segmental construction has increased in recent years due to the demand for shortened construction periods and the desire for innovative designs that yield safe, economical and efficient structures.[1,2]

As precast post-tensioned segments are being more widely used for the construction of floors, roofs, and frames, it was thought that information regarding the shear strength of joints between two such segments might be of interest.

Joints between precast post-tensioned segments require special attention when designing and constructing precast segmental structures. These joints must transmit the large compressive, shear and sometimes tensile stresses that may develop in the joint locations.

Segments are generally mortared together and then post-tensioned, but often, owing to shrinkage or other causes, the bond between segments is broken, leaving only friction between surfaces to prevent slipping.

The shear transference across open joints is a more complex matter. The universally accepted theory for evaluating the shear strength of joints considers the shear stresses to be transferred across the joint through complex mechanisms. The mechanism represents the friction resistance that arises when two flat and compressed surfaces attempt to slide one against the other; this resistance is proportional to the actuating compression, and the corresponding proportionality factor is the friction coefficient.[3]

[1)]KCI member, Civil Engineering Research Team, Daewoo Institute of Construction Technology, Suwon. 440-210, Korea.
[2)]Dept. of Civil and Environmental Engineering, Sungkyunkwan University, Suwon. 440-746, Korea. *E-mail address: hmshin@skku.ac.kr*

A numerical study on the joints between precast post-tensioned segments is presented in this paper. Other authors[3,4] have presented numerical studies on the joints between precast post-tensioned segments. However, more information on this joint is required and necessary, especially for more detailed strength checks and comprehensive design guidelines.

The principal objective of this study is to provide detailed knowledge on the joints between precast post-tensioned segments. Previous formulations for joint elements are reviewed and a suitable method is selected for this study. A material model is proposed for the behavior of joints, and the implementation in the finite element program is discussed.

The proposed method, uses a nonlinear finite element analysis program (RCAHEST, reinforced concrete analysis in higher evaluation system technology), developed by the authors.[5-8] A joint element is newly incorporated into the structural element library for RCAHEST so that it can be used to predict the inelastic behavior of segmental joints.

2. Nonlinear material model

The nonlinear material model for the prestressed concrete is composed of models to characterize the behavior of the concrete, in addition to models for characterizing the reinforcing bars and tendons (see Fig. 1).

The models for concrete may be composed of the models for uncracked concrete and cracked concrete. The basic model adopted for crack representation is a non-orthogonal fixed-crack method of the smeared crack concept, which is widely known to be a model for crack representation. This approach is practical for cyclic loads where the load history needs to be recorded.

This section includes summaries of the material models used in the analysis. A full description of the nonlinear material model

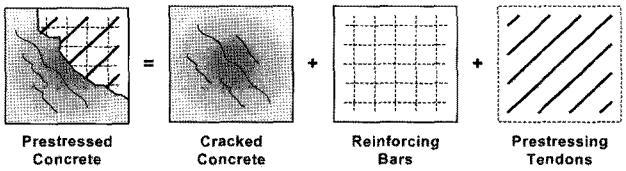

Fig. 1 Prestressed concrete material model.

for reinforced concrete is given by Kim et al.[6-8]

2.1 Models for uncracked and cracked concrete

The widely used elasto-plastic and fracture model for the biaxial state of stress proposed by Maekawa and Okamura[9] is used as the constitutive equation for the uncracked concrete. For uncracked concrete, the nonlinearity, anisotropy, and strain softening effects are expressed independently of the loading history.

After concrete cracks, the behavior becomes anisotropic in the crack direction. The stress-strain relations are modeled by being decomposed in directions parallel to, along and normal to cracks, respectively. Thus, the constitutive law adopted for the cracked concrete consists of tension stiffening, compression stiffness and shear transfer models.

Cracked concrete may resist a certain amount of tensile stress normal to the cracked plane because of the bond effect between the concrete and the reinforcing bars. A refined tension stiffening model is obtained by transforming the tensile stresses of concrete into the component normal to the crack, and improved accuracy is expected, especially when the reinforcing ratios in orthogonal directions are significantly different and when the reinforcing bars are distributed only in one direction. For the tension stiffening model for unloading and reloading, the model proposed by Shima et al.[10] is used.

A modified elasto-plastic fracture model is used to describe the compressive behavior of concrete struts in between cracks in the direction of the crack plane. The model describes the degradation in compressive stiffness by modifying the fracture parameter in terms of the strain perpendicular to the crack plane. Cyclic load causes damage to the inner concrete and energy is dissipated during the unloading and reloading processes. This behavior is considered in the model by modifying the stress-strain curve at unloading to an experimentally fitted quadratic curve.

The shear transfer model based on the contact surface density function[11] is used to consider the effect of shear stress transfer due to the aggregate interlock at the crack surfaces. The contact surface is assumed to respond elasto-plastically and the model is applicable to any arbitrary loading history. For unloading and reloading, the shear transfer model modified by the authors[6] is used.

2.2 Model for the reinforcing bars in concrete

The stress acting on the reinforcing bar embedded in concrete is not uniform and the value is maximum at locations where the bar is exposed to a crack plane. The constitutive equations for the bare bar may be used if the stress-strain relation is in the elastic range. The post-yield constitutive law for the reinforcing bar in concrete considers the bond characteristics and the model is a bilinear model. Kato's model[12] for the bare bar under the reversed cyclic loading and the assumption of stress distribution denoted by a cosine curve were used to derive the mechanical behavior of reinforcing bars in concrete under the reversed cyclic loading.

For reinforcing bars under extreme compression, lateral bar buckling tends to occur, which greatly affects the post peak behavior and member ductility. To account for buckling of reinforcing bars, the average stress-strain behavior after concrete crushing is assumed to be linearly descending until the 20% of the average steel stress. This relation was derived from a parametric study using finite element analysis.[7]

2.3 Model for the prestressing tendons in concrete

The bilinear curve used to characterize the mild steel behavior, showing a brusque yielding, is not immediately extrapolable to prestressing tendons. For prestressing tendons, which does not have a definite yield point a multilinear approximation may be required. High strength steel used for prestressing shows a rather large proportional behavior followed by a progressive yielding. To simulate such a behavior, Kang[13] and Mari[14] used a multilinear curve of five branches. In this study, the modified modeling is adopted for the present formulation as follows (see Fig. 2).

A trilinear model for the stress-strain relationship of prestressing tendon has been used. Unloading and reloading processes are accounted for through straight branches with the initial modulus.

$$\sigma_{pt} = f_{py} + E_{ph1}(0.03 - \varepsilon_{py}) + E_{ph2}(\varepsilon_{pu} - 0.03) \tag{1}$$

$$E_{ph1} = \frac{f_{0.03} - f_{py}}{0.03 - \varepsilon_{py}} \tag{2}$$

$$E_{ph2} = \frac{f_{pu} - f_{0.03}}{\varepsilon_{pu} - 0.03} \tag{3}$$

where σ_{pt} = stress of tendon; f_{py} = yield strength of tendon; f_{pu} = ultimate strength of tendon; ε_{py} = yield strain of tendon; ε_{pu} = ultimate strain of tendon; and E_{ph1}, E_{ph2} = strain hardening rates of the tendon embedded in concrete.

3. Model for joints

In the joint model, the inelastic behavior of the joint elements

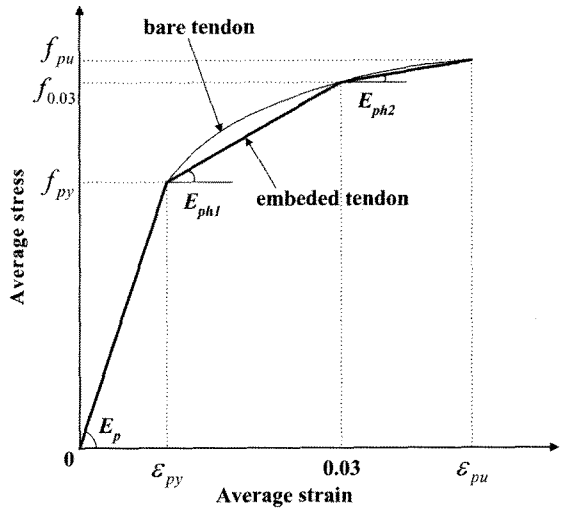

Fig. 2 Model for prestressing tendons.

is governed by normal and tangential stiffness coefficients. These relate the normal and tangential stresses of the joint to the normal and tangential relative displacements between the joint faces.[15] The state of stress beyond which yielding starts is defined by the yield surface, and the behavior of the joint after yielding is governed by the potential yield surface.[16]

3.1 Behavior before failure

A material law is formulated which models the experimentally obtained data for adhesive joints in concrete. The material properties differ substantially in the two main directions (along the joint element and perpendicular to the element) (see Fig. 3).

In the local "1" axis the joint element exhibits the axial properties of either the joint material or the adjacent material. In the local "2" axis the joint behavior is governed by the characteristics of the interface between these two materials, or either one of these materials. Due to the lack of experimental data, it is assumed that the behavior of the joint in the two directions can be uncoupled in such a way that the behavior in the "1" direction can be treated as purely uniaxial. In the direction of the "2" axis the joint is also treated uniaxially, but some interaction exists between this directions and shear along the joint element.

Since the joint element is very small with respect to the surrounding elements, linear elastic stress-strain relations can be used before failure without significantly affecting the behavior of the structure as a whole. It is also assumed that prior to failure the joint is elastic, and that the post-failure behavior is governed by the particular mode of failure.

If one of the materials exceeds its failure strength, the modulus of elasticity can either drop to zero, or become negative (in a strain-softening material). If the thickness of that material is negligible with respect to other material, the effect on the total effective stiffness could be small.

3.2 Post failure behavior

It is assumed that under tensile loads the material fails in a brittle manner in both direction, while the joint yields in a perfectly plastic manner under compressive loads. After failing in shear it is also assumed that the joint is plastic. Experimental evidence indicates that the failure of this material can be described by a Coulomb type relation (see Fig. 4),

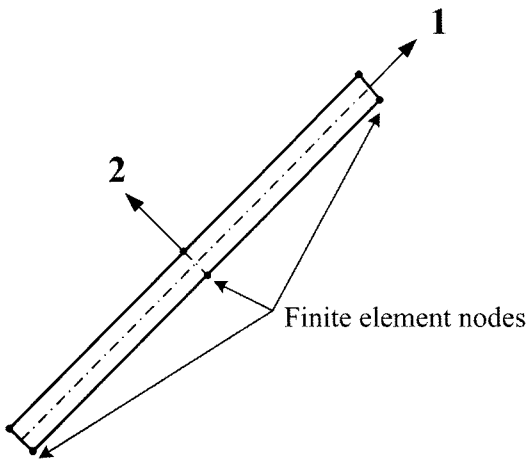

Fig. 3 Definition of axis in joint element.

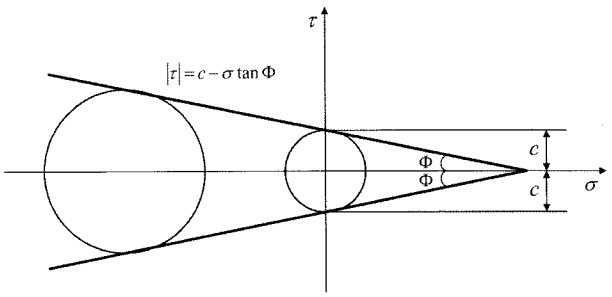

Fig. 4 Coulomb failure criterion.

$$f_{sk} = c - \sigma \tan\Phi \tag{4}$$

where f_{sk} = shear transfer strength due to Coulomb criterion; σ = normal stress at the joint; Φ = angle of internal friction; and c = cohesion.

The shear stress model based on the contact surface density function[11] is used to consider the effect of shear stress transfer (see Fig. 5). For finite element computation, a shear softening is added to the envelope of shear stress model. In the model, the shear stress at the joint is calculated using the following equations:

1) Loading

$$\tau_{xy} = K_{shro}\gamma_{xy} \tag{5}$$

2) Unloading and reloading ($\beta \geq 0$)

$$\tau_{\max} = f_{sk}\frac{\beta_{\max}^{\ 2}}{(1+\beta_{\max}^{\ 2})} \tag{6}$$

$$\tau_{xy} = \tau_{\max}\left(\frac{\beta}{\beta_{\max}}\right)^3 \tag{7}$$

3) Unloading and reloading ($\beta < 0$)

$$\tau_{\min} = f_{sk}\frac{\beta_{\min}^{\ 2}}{(1+\beta_{\min}^{\ 2})} \tag{8}$$

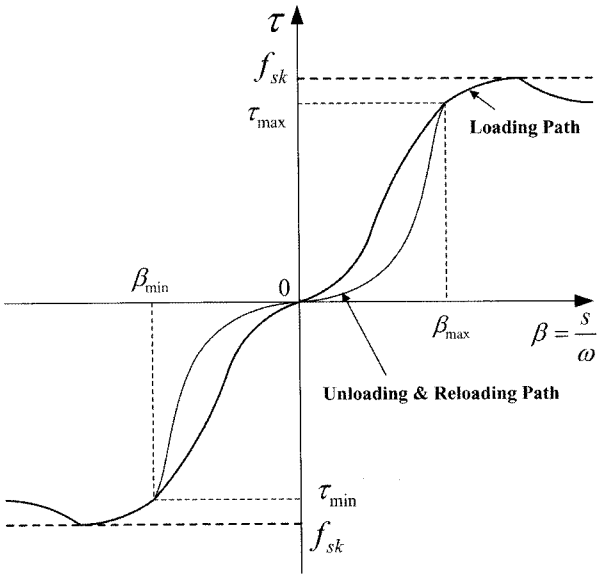

Fig. 5 Shear stress model.

$$\tau_{xy} = -\tau_{\min}\left(\frac{\beta}{\beta_{\min}}\right)^3 \quad (9)$$

where τ_{xy} = shear stress at the joint; K_{shro} = shear stiffness at the joint; γ_{xy} = shear strain at the joint; β = normalized shear strain (= s/w); s = slip displacement at the joint; w = opening displacement at joint (> 0.000001), $\tau_{\max}$ = maximum shear stress in envelope curve; f_{sk} = shear transfer strength due to Coulomb criterion; $\beta_{\max}$ = maximum normalized shear strain in envelope curve; $\tau_{\min}$ = minimum shear stress in envelope curve; and $\beta_{\min}$ = minimum normalized shear strain in envelope curve.

3.3 Implementation of the finite elements

The material model described above is implemented in a two-dimensional (plane stress) finite element (see Fig. 6).

An orthotropic formulation is used to accommodate the different properties in each of the main directions. The strain is calculated at each integration point, and the corresponding stresses and stiffnesses are then calculated accordingly. The stiffness and load vector of the isoparametric finite element are complied in the usual way.

4. Nonlinear finite element analysis program RCAHEST

RCAHEST is a nonlinear finite element analysis program for analyzing reinforced concrete structures.[5] The program is used to model various reinforced concrete structures under a variety of loading conditions.

The proposed structural element library RCAHEST is built around the finite element analysis program shell named FEAP, developed by Taylor.[17] FEAP is characterized by modular architecture and by the facility that is used to introduce the type of custom elements, input utilities, and custom strategies and procedures.

Accompanying the present study, the authors attempt to implement an unbonded tendon element[18] and a newly developed joint element.

Highly iterative procedure is required to analyze the regions of unbonded tendon. Complex iterative procedures are needed to satisfy the displacement compatibility between concrete and unbonded tendon at the anchorage because of interactions between concrete and unbonded tendon. The analysis of unbonded tendon was also found to be susceptible to convergence problems and some considerable effort was spent in developing program methodologies to provide efficient solutions.[18]

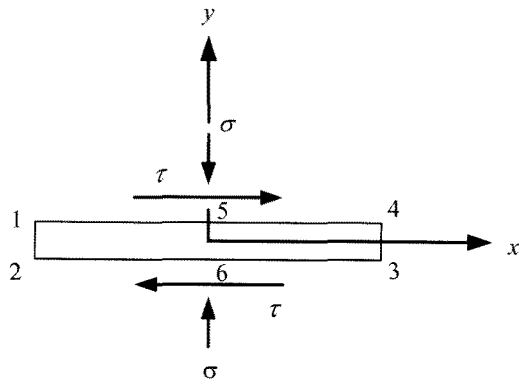

Fig. 6 Joint element.

5. Numerical examples

5.1 Description of test specimens

The data for the joints between precast post-tensioned segments by Jones[19] were used to verify the applicability of the proposed method.

The individual segments, of which two were joined together to form a test beam, were 3 ft 6 in. long, 6 in. deep, and 4 in. wide with a longitudinal central hole of 7/4 in. diameter (see Fig. 7).

Tests have been carried out on post-tensioned members having the following types of joints: series A plain butt; series B mortared. As it was anticipated that the plain butt and mortared joints would fail by slipping, the test beam was made long enough to prevent buckling of the tendon when such slipping occurred.

After stressing, the test beam was placed and tested in a standard 50 ton machine, series A and B being supported as shown in Fig. 8. Units of series A were merely butted together while those of series B were joined together with mortar 1/2 in. thick between units.

More detailed descriptions of scheme are available in Reference.[19]

5.2 Description of analytical model

Fig. 9 shows the finite element discretization and the boundary conditions for analysis of precast post-tensioned segments. The joint elements enhance the modeling of the effects of the slip displacement and opening displacement. The unbonded tendon element was also used to describe the inelastic behaviors of unbonded prestressing tendon.

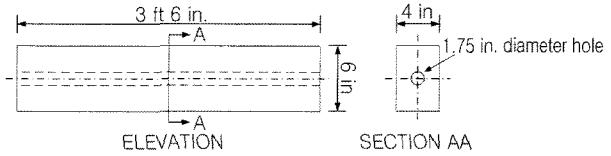

Fig. 7 Details of test specimen. (1 in. = 25.4 mm)

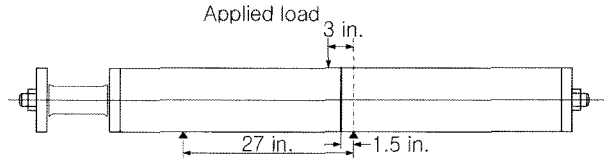

Fig. 8 Plain butt joints and mortared joints test. (1 in. = 25.4 mm)

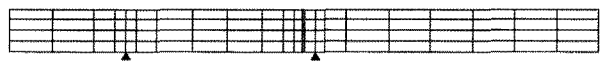

8-node Plane stress element	84
6-node Joint element	4
n-node Unbonded prestressing element	1

Fig. 9 Finite element mesh for specimens.

5.3 Comparison with experimental results

The value given by all specimens were similar with the analytical results; comparative data are summarized on Tables 1 and 2. In predicting the results of the series, under a variety of prestressing forces, the mean ratios of experimental-to-analytical shear strength were 1.03 at a COV of 1%.

A larger axial load was then applied, and the shear stress was increased until the joint slipped again. Since failure occurred by

Table 1 Experimental and analytical results on plain butt joints.

Prestressing force (tons)	Prestress (lb/in^2)	Load (tons)	Shear force / Prestressing force (μ)	Shear force at joints (tons)		
				Exp. (1)	Ana. (2)	(1)/(2)
0.96	100	0.45	0.417	0.40	0.40	1.00
1.12	116	0.71	0.572	0.64	0.62	1.03
1.20	125	0.53	0.391	0.47	0.47	1.00
2.04	212	1.04	0.456	0.93	0.91	1.02
2.08	216	1.21	0.514	1.07	1.04	1.03
2.30	238	1.31	0.505	1.16	1.13	1.03
3.60	363	2.45	0.606	2.18	2.10	1.04
3.74	388	2.24	0.532	1.99	1.92	1.04
3.89	402	2.66	0.606	2.36	2.27	1.04
4.24	440	2.58	0.540	2.29	2.21	1.04
5.40	560	3.25	0.535	2.89	2.78	1.04
5.41	561	3.21	0.527	2.85	2.75	1.04
5.65	586	4.15	0.654	3.69	3.56	1.04
5.80	601	3.44	0.528	3.06	2.95	1.04
5.90	612	3.15	0.474	2.80	2.71	1.03
5.95	616	2.96	0.442	2.63	2.56	1.03
8.30	860	4.57	0.488	4.06	3.92	1.04
8.45	875	5.15	0.542	4.58	4.41	1.04
8.55	886	4.88	0.508	4.34	4.19	1.04
8.70	902	6.05	0.618	5.38	5.17	1.04
10.00	1,036	5.70	0.506	5.06	4.94	1.02
11.10	1,150	5.70	0.456	5.06	4.91	1.03
11.45	1,185	6.75	0.524	6.00	5.78	1.04
11.50	1,192	8.07	0.625	7.18	6.92	1.04
11.60	1,203	7.29	0.560	6.48	6.24	1.04
15.30	1,585	9.70	0.565	8.64	8.29	1.04
15.42	1,600	9.74	0.559	8.62	8.27	1.04
15.45	1,602	8.42	0.484	7.48	7.22	1.04
15.50	1,605	10.12	0.581	9.00	8.64	1.04
15.90	1,647	8.15	0.457	7.25	7.04	1.03
18.60	1,925	10.80	0.516	9.60	9.25	1.04
19.10	1,980	14.82	0.691	13.20	12.78	1.03
19.70	2,041	10.30	0.464	9.15	8.84	1.04
19.80	2,050	12.50	0.562	11.12	10.67	1.04
24.50	2,540	12.60	0.457	11.20	10.84	1.03
27.90	2,890	14.15	0.452	12.58	12.21	1.03
Mean	-	-	-	-	-	1.03
COV	-	-	-	-	-	1.01

Note: 1 tons = 9.81 kN, 1 $lb/in^2 = 6.89 \times 10^{-3}$ MPa.

Table 2 Experimental and analytical results on mortared joints.

Prestressing force (tons)	Prestress (lb/in^2)	Load (tons)	Shear force / Prestressing force (μ)	Shear force at joints (tons)		
				Exp. (1)	Ana. (2)	(1)/(2)
5.40	559	4.63	0.763	4.12	4.03	1.02
9.70	1,003	7.25	0.665	6.45	6.23	1.04
14.30	1,480	10.37	0.645	9.22	8.89	1.04
Mean	-	-	-	-	-	1.03
COV	-	-	-	-	-	1.01

Note: 1 tons = 9.81 kN, 1 $lb/in^2 = 6.89 \times 10^{-3}$ MPa.

slipping of surfaces it was possible for a specimen to be tested repeatedly, provided that only a small slip was allowed to take place. Since these structures are very susceptible to the prestressing level, such that an increase of the prestressing force permits one to notably increase the safety factor.

The results have been plotted showing the relation between the prestressing force and the shear force across the joint (see Fig. 10). It was assumed that the frictional force was the only force resisting shear and values of coefficients of friction (μ) have therefore calculated.

It is clear that B series of tests the shear strength of the joints was the sum of the bond strength of the mortar and the frictional force developed. It can be seen that, as might have been expected, for similar values of the prestress the shear strength was much higher in series B than in series A.

In general, the results of the analytical model presented herein correlated reasonably well with the experimentally observed behavior of the joints between precast post-tensioned segments.

6. Conclusions

The proposed method provides a rational and systematic framework for evaluating the inelastic behavior of joints between precast post-tensioned segments.

This study also evaluated the shear strength of joints as influenced by the applied normal stress, the size of the contact area, and the conditions of two surfaces. The analytical results obtained with prestressing force as analytical input data provided a better match with the experimental results.

The failure mechanism for all tests conducted in this study was a shear friction failure. Analyses of the results of tests on the frictional behavior of joints revealed that the design criteria seem to be rather conservative. The data also manifested that the surface preparation and the size of the contact area did not seem to influence the shear strength of such a joint.

Joints between precast post-tensioned segments affect the structural failure behavior of the precast segments. Available test results including this study are not sufficient to draw firm conclusions. Further research is therefore needed to provide a better understanding of the behavior of these joints. Nevertheless, a new series of tests has been initiated in this study to investigate the behavior and failure of the joints.

It is apparent from this study that many aspects regarding the behavior of concrete and precast segmental bridge columns need further investigation and verification.

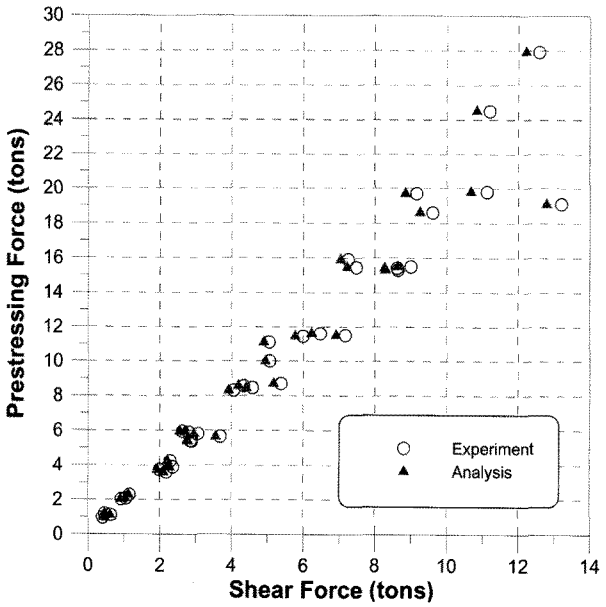

Fig. 10 Comparison between experimental and analytical results (1 tons = 9.81 kN).

References

1. Billington, S. L., Barnes, R. W., and Breen, J. E., "Alternative Substructure Systems for Standard Highway Bridges," *Journal of Bridge Engineering*, ASCE, Vol.6, No.2, 2001, pp.87~94.

2. Nasir, S., Gupta, S., Umehara, H., and Hirasawa, I., "An Efficient Method for the Construction of Bridge Piers," *Engineering Structures*, Vol.23, No.9, 2001, pp.1142~1151.

3. Turmo, J., Ramos, G., and Aparicio, A. C., "FEM Study on the Structural Behaviour of Segmental Concrete Bridges with Unbonded Prestressing and Dry Joints: Simply Supported Bridges," *Engineering Structures*, Vol.27, 2005, pp.1652~1661.

4. Ong, K. C. G., Hao, J. B., and Paramasivam, P., "Flexural Behavior of Precast Joints with Horizontal Loop Connections," *ACI Structural Journal*, Vol.103, No.5, 2006, pp.664~671.

5. Kim, T. H. and Shin, H. M., "Analytical Approach to Evaluate the Inelastic Behaviors of Reinforced Concrete Structures under Seismic Loads," *Journal of the Earthquake Engineering Society of Korea*, EESK, Vol.5, No.2, 2001, pp.113~124.

6. Kim, T. H., Lee, K. M., Yoon, C. Y., and Shin, H. M., "Inelastic Behavior and Ductility Capacity of Reinforced Concrete Bridge Piers under Earthquake. I: Theory and Formulation," *Journal of Structural Engineering*, ASCE, Vol.129, No.9, 2003, pp.1199~1207.

7. Kim, T. H., Lee, K. M., Chung, Y. S., and Shin, H. M., "Seismic Damage Assessment of Reinforced Concrete Bridge Columns," *Engineering Structures*, Vol.27, No.4, 2005, pp.576~592.

8. Kim, T. H., Kim, B. S., Chung, Y.-S., and Shin, H. M., "Seismic Performance Assessment of Reinforced Concrete Bridge Piers with Lap Splices," *Engineering Structures*, Vol.28, No.6, 2006, pp.935~945.

9. Maekawa, K. and Okamura, H., "The Deformational Behavior and Constitutive Equation of Concrete Using Elasto-Plastic and Fracture Model," *Journal of the Faculty of Engineering, University of Tokyo (B)*, Vol.37, No.2, 1983, pp.253~328.

10. Shima, H., Chou, L., and Okamura, H., "Micro and Macro Models for Bond Behavior in Reinforced Concrete," *Journal of the Faculty of Engineering, University of Tokyo (B)*, Vol.39, No.2, 1987, pp.133~194.

11. Li, B., Maekawa, K., and Okamura, H., "Contact Density Model for Stress Transfer across Cracks in Concrete," *Journal of the Faculty of Engineering, University of Tokyo (B)*, Vol.40, No.1, 1989, pp.9~52.

12. Kato, B., "Mechanical Properties of Steel under Load Cycles Idealizing Seismic Action," *CEB Bulletin D'Information*, Vol.131, 1979, pp.7~27.

13. Kang, Y. J., *Nonlinear Geometric, Material and Time Dependent Analysis of Reinforced and Prestressed Concrete Frames*, University of California, Berkeley, UC-SESM Report

No.77-1, 1977.

14. Mari, A. R., *Nonlinear Geometric, Material and Time Dependent Analysis of Three Dimensional Reinforced and Prestressed Concrete Frames*, University of California, Berkeley, UC-SESM Report No.84-12, 1984.

15. Maekawa, K., Pimanmas, A., and Okamura, H., *Nonlinear Mechanics of Reinforced Concrete*, SPON Press, 2001.

16. Chen, W. F. and Han, D. J., *Plasticity for Structural Engineers*, Springer-Verlag, 1988.

17. Taylor, R. L., *FEAP-A Finite Element Analysis Program, Version 7.2 Users Manual*, Vol.1 and Vol.2, 2000.

18. Kim, T. H., Park, J. G., Jin, B. M., and Shin, H. M., "Analytical Study on the Inelastic Behavior of Reinforced Concrete Bridge Columns with Unbonded Tendons," *Journal of the Korean Society of Civil Engineers*, Vol.25, No.5A, 2005, pp.813~821.

19. Jones, L. L., "Shear Tests on Joints between Precast Post-Tensioned Units," *Magazine of Concrete Research*, Vol.11, No.31, 1959, pp.25~30.